FLIGHT SIMULATION MODEL OF A MULTI-FIDELITY DIGITAL TWIN OF AN EVTOL DRONE

Andrea Pedrioli, Zurich University of Applied Science, Switzerland
Andrea Vaiuso, Zurich University of Applied Science, Switzerland
Noé Pedrazzini, Zurich University of Applied Science, Switzerland
Oier Coretti, Zurich University of Applied Science, Switzerland
Elena Garcia Sanchez, European Union Aviation Safety Agency, Germany
Laurent Pinsard, European Union Aviation Safety Agency, Germany
Joana Vieira Gomes, European Union Aviation Safety Agency, Germany
Pierluigi Capone, Zurich University of Applied Science, Switzerland
Marcello Righi, Zurich University of Applied Science, Switzerland

Abstract

In the last decade, novel advancements in electric motors have revived the possibility of developing new VTOL airplanes. While their potential is clear, significant engineering challenges remain. The goal of this study was to test different advanced modeling and simulation techniques, including both physics-based and data-driven approaches. This work is part of the MODEL-SI project, where a previous contribution reviewed applicable methods for the development of an eVTOL Digital Twin (DT). A modular approach was chosen to build a comprehensive Flight Simulation Model (FSM). Conventional physics-based methodologies were primarily used, while some modules were implemented using a state-of-the-art, i.e. Co-Kriging, and a novel Machine Learning (ML) method: the Bayesian Neural Network with Transfer Learning (BNN-TL). An initial assessment between the two methods demonstrated the superior capabilities of BNN-TL in handling complex problems. Ultimately, the final FSM is capable of performing static and dynamic analyses, such as aircraft trim, transition simulation, and aeroelastic analyses.

NOTATION

Symbols

δ_{DE}	Elevator deflection, deg
f	Frequency, Hz
N	Rotational speed, rpm
M_B	Bending Moment, N·m
TAS	True Airspeed, m/s
T	Propeller thrust, N
Q	Propeller torque, N·m
U	Velocity, m/s

Acronyms

AOA	Angle Of Attack
AOS	Angle Of Sideslip
AP	Airplane
BEM	Blade Element Method
BNN	Bayesian Neural Network
CFD	Computational Fluid Dynamics
DT	Digital Twin
EASA	European Union Aviation Safety Agency
eVTOL	electrical Vertical Take Off and Landing
FCS	Flight Control System
FEM	Finite Elements Method
FSM	Flight Simulation Model
FT	Flight Test
GP	Gaussian Process
HC	Helicopter
HF	High-Fidelity
LCO	Limit Cycle Oscillations
LF	Low-Fidelity
MF	Mid-Fidelity
ML	Machine Learning
RMS	Root Mean Square
RPM	Revolutions per Minute
TL	Transfer Learning
UQ	Uncertainty Quantification
VLM	Vortex Lattice Method
VPM	Vortex Particle Method

1. INTRODUCTION

The advantages of an aircraft capable of both vertical take-off and landing, as well as horizontal flight using wings, are evident. However, the engineering obstacles associated with such vehicles are not trivial. Vertical Take-Off and Landing (VTOL) airplane have been designed since the early days of aviation, yet only a handful have achieved successful and reliable flight. The recent advancements in reliable and efficient electric motors have prompted manufacturers to reimagine VTOL designs by replacing traditional combustion engines with their electric counterparts. This technology advancement opened the doors to innovative configurations, like distributed propulsion and simpler tiltable mechanisms, but introduced as well new challenges and unknown uncertainties. For example, the aerodynamic and structural interaction between the various rotors and wings could be more complex than in a standard airplane or helicopter. Therefore to ensure reliable and safe operations, the certification process can be strenuous.

This paper is part of the MODEL-SI project, funded by the Horizon Europe and managed by the European Union Aviation Safety Agency (EASA), and it is investigating the aforementioned challenges by carrying out a case study. The primary goal of this study is to explore and assess advanced modeling and simulation techniques, using both physics-based and data-driven approaches. A Digital Twin (DT) can potentially reduce time and computational costs by maintaining High-Fidelity (HF) predictions. The aim is to facilitate complex eVTOL design and development and to support challenges associated with certification and continued airworthiness.

A first work was presented during a prior conference (Ref. [1]). The authors summarized standard aerospace methods for modeling a complete eVTOL aircraft with varying fidelity levels, from Low-Fidelity (LF), such as lifting-line theory, to HF, e.g. with Computational Fluid Dynamics (CFD) simulations. From the initial research, a trend to use LF methods for structural modeling and HF methods for aerodynamics and rotor dynamics is noted. Additionally, a series of methodologies for implementing a comprehensive Flight Simulation Model (FSM) framework is proposed, offering a total analysis of system responses, from a structural and Flight Control System (FCS) point of view. A preliminary example of a surrogate model of a rotor-wing-rotor system was presented, which applies most of the methods proposed.

This paper can be divided into two main parts: the former is about the implementation of the methods proposed in Ref. [1] to build a complete FSM eVTOL airplane, while the latter is on the data-driven model implementation and its integration in the FSM. To properly address and predict the complex rotor-wing interaction, Mid-Fidelity (MF) and HF aerodynamics methods could be exploited, namely using the Vortex Particle Method (VPM) and CFD. In the last few years, VPM has increased in popularity thanks to its promising prediction capabilities of complex systems (Ref. [2]). Vortical flows are effectively modelled with reasonable computational costs. However, it is still limited to low angle of attack (AOA) cases. An important difference between the two approaches lies in the computational costs of a 3D simulation of a complete eVTOL, which could also be measurable in one order of magnitude. To take advantages from this data, Machine Learning (ML) is exploited by means of Gaussian Processes (GP) and Bayesian Neural Networks (BNN) with Transfer Learning (TL). While the former method is well-known in the aerospace industry and considered state-of-the-art, the latter is an interesting alternative to cope with complex systems. The approach combines the advantages of data fusion and the assessment of predictive uncertainties in a single method. As shown in the work of Vaiuso et al. (Ref. [3]), BNN-TL seems to be a promising alternative to GPs.

In order to effectively test our methods, both physics-based and data-driven, a real flying machine is chosen. The eVTOL selected is the Skiron Expeditionary (Skiron-X) from Aurora Flight Sciences, a Boeing Company. It is operated by Aurora with a simple configuration equipped with static lift and cruise propellers. The air vehicle has been developed to easily takeoff and land vertically and to perform sustained endurance fixed-wing flights. The vehicle length and wingspan are about 2.2 and 5 m, respectively, and weighs 22 kg. It can fly at a maximum forward speed of 26 m/s and offers an endurance of 3 hours in fixed-wing flight. As can be seen in Figure 1, it has four longitudinal-symmetrical placed propellers, in front and behind the wing, which serve as lift devices for Helicopter (HC) mode related activities, such as takeoff/landing, hovering and ascent/descent. Additionally, a pusher propeller is attached behind the vehicle's tail, and it is used in Airplane (AP) mode as a forward thrust device.

Figure 1: Skiron-X eVTOL drone of Aurora Flight Sciences.

2. METHODOLOGY

To assess the eVTOL behavior in various nominal and failure conditions over the entire flight envelope, a comprehensive flight simulation framework is needed. Many implementation techniques are possible and since the physics complexity is not straightforward, a flexible and modular approach is chosen.

2.1. Flight Simulation Model Architecture: Modular approach

The final FSM is a comprehensive software composed of modules interconnected with each other. Various simulations can be performed, from a flight mechanics to an aeroelastic point of view. For example, one can trim the eVTOL in various conditions and analyze if the system structure is stable. It is extremely helpful in understanding harmful flight regimes which could cause instabilities, such as flutter.

Each module is developed initially with a physics-based LF model and it treats a single field, such as steady aerodynamics. The modular approach allows to modify, therefore to improve or replace, each module separately. For example, one could decide to increase the fidelity of the steady aerodynamics by keeping a LF level of the structure. In addition, and more interesting within the scope of this project, is the possibility of replacing one or multiple modules with a data-driven model.

The FSM structure is shown in Figure 2, where the main two blocks are depicted in blue, i.e. the Flight Mechanics and Aeroelastic modules. Both elements depend on the FSM inputs, which are the definition of the desired analysis. For example, it could be the definition of an operating point for trim calculation and linear stability analysis. In addition, and to introduce proper environmental conditions, turbulence, wind and gust were modeled based on the Dryden form of the spectra for the turbulence as described in Ref [4].

The Quasi-Steady Aerodynamics module is implemented through classical approaches (Ref. [5]): wing and tail aerodynamics were modeled with a classical Vortex Lattice Method (VLM), while the fuselage accounted only for the parasitic drag. Propellers forces and moments were approximated via an actuator disk model (Ref. [6]) and corrected with a uniform inflow model (Ref. [7]). In addition, the dynamics of the propeller rotation were also taken into account. It should be noted that this methodology is considered LF because there is no interaction between the propeller, wing and tail aerodynamics.

To model the aircraft structure, the Finite Element Method (FEM) was chosen (Ref. [8]). The eVTOL was broken down into interconnected finite elements, such as beams and nodes, each characterized by distinct properties like stiffness and inertia. The structural dynamics module is composed of the FEM structure, which is optimized with the modal condensation technique. Geometric nonlinearity can be taken into account in the static solution.

The Flight Control System (FCS) is composed of the eVTOL flight control computer, sensor and actuator models. While the latter two are modeled as simple low-pass filters, the flight controller is divided into two sets of cascaded PID control loops. In HC mode, the primary loop regulates the vehicle attitude by adjusting the throttle of the four hover propellers. When transitioning to AP mode, a separate loop takes control, utilizing the pusher propeller and aerodynamic control surfaces.

On the other hand, the Aeroelastic module focuses on the interaction between aerodynamic forces and structural dynamics within the flexible structures, such as the eVTOL wings and propeller blades. It was found that the rigid body modes and the elastic ones are sufficiently well separated in frequency. This granted to treat separately the Flight Mechanics and Aeroelastic modules. The resulting structural deformations and vibrations occur during flight operations due to aerodynamic loads acting on the aircraft. Aeroelastic phenomena encompass a variety of behaviors that can significantly impact the eVTOL performance and safety. Examples include flutter, divergence, control reversal, and gust response. Therefore, a deep understanding and mitigation of these effects is paramount to ensuring safe and reliable operations. The Aeroelastic module relies on steady and unsteady formulations. The former takes advantage from a multi-fidelity surrogate model to estimate propeller thrust and potentially wing lift and drag values.

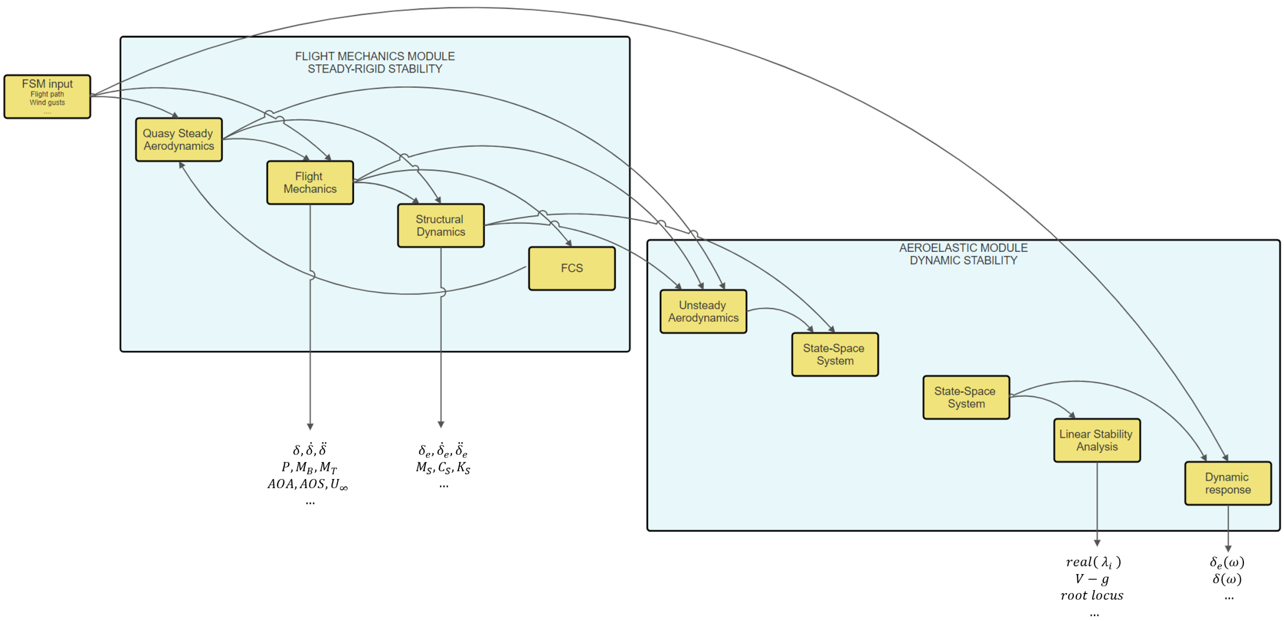

Figure 2: FSM architecture diagram composed by the Flight Mechanics and Aeroelastic modules.

This part is inherently non-linear due to the physics involved that need to be captured. The latter unsteady part requires a dedicated approach to account for aerodynamic lag, but it was considered as a linear contribution.

The flowchart depicted in Figure 2 indicate as well a state-space formulation, which is based on a time-domain approach and derived from Theodorsen theory (Refs. [9] and [10]). This distinction reflects the conventional approach to aeroelastic analysis in fixed-wing aircraft, where static aeroelastic solutions are non-linear and stability analysis relies on a linearized formulation (Ref. [11]). The Aeroelastic module outputs dynamic response in time and frequency domain as well as the dynamic stability margins obtained from the linearized system. Finally, a dynamic response can be obtained to study the aircraft behavior in transient and dynamic conditions.

2.2. Multi-fidelity modeling

This section describes the development of a data-driven model for all five eVTOL propellers, which is subsequently integrated into the FSM. Utilizing multi-fidelity modeling approaches has the potential to significantly improve the accuracy of the FSM predictions.
The most important physical phenomenon to consider is the interaction between the rotors and the wing. The wakes generated by the two front rotors significantly impact the airflow over the wing and the rear rotors. This wake impingement modifies the wing's lift distribution, potentially introducing dynamic loading and increasing drag. Additionally, the control surface effectiveness is reduced on the portion of the wing impacted by the wake. As highlighted in Ref. [1], the rear rotor also experiences a negative effect, generating less thrust compared to the front rotor for the same power input. Conversely, once the wing starts generating lift, the nearby flow field is distorted, causing a curvature in front of the leading edge. This curvature can also affect the performance of the front rotor depending on its position.

2.2.1. Physics-based models

To build a multi-fidelity model, physics-based datasets with different fidelities are needed. Here the data-driven model relies on LF and MF methods.

Low-fidelity model

The LF model takes advantage of a classical approach. A linear inflow model is coupled to a BEM to take into account the inlet flow speed changes caused by the rotor rotation (Ref. [12]). Each computation is extremely fast and it could be used even for real-time simulations.

Mid-fidelity model

On the other hand, MF calculations are performed using the VPM. This approach allows to capture the complex interactions between the wing and rotors, as well as rotor-to-rotor interactions. The MF dataset is generated with DUST (Ref. [13]), an open-source code based on VPM. Skiron-X external aerodynamics have been completely modeled with this approach, including all five rotors, the wing, ruddervators, and fuselage. Figure 3 shows an example of the DUST simulation output for Skiron-X during a transition. The figure depicts the pressure coefficient on the eVTOL wings, while the gray spheres describe the vorticity magnitude. As shown, the rear rotor is completely immersed in the wake generated by the front rotor and the wing. This wake interaction reduces the thrust of the rear rotor even though it operates at the same rotational speed as the front rotor.

2.2.2. Machine Learning

The implementation of a data-driven model involves ML techniques and in particular it leverages data fusion. Our approaches rely on the work conducted by Vaiuso et. al (Ref. [3]), where the state-of-the-art Co-Kriging and a novel Bayesian Neural Network (BNN) with Transfer Learning (TL) are employed:

- GPs are exploited thanks to the Co-Kriging technique. It has the advantage of being relatively simple to implement and interpret. For simple cases, the correlation between datasets of different fidelity can be well captured. In addition, the variance and covariance estimates obtained can be harnessed to quantify the epistemic uncertainty, which reflects the inherent limitations in our knowledge of the underlying system (Ref. [14]).
- The second ML approach has two key objectives. Firstly, to fuse the data of different fidelity together through the so-called Transfer Learning (Ref. [15]). The method is used to transfer the weight values to the highest-fidelity deep neural network, followed by a continuous training based only on HF data. Eventually, some neurons are frozen and a fine-tuning is performed to optimize the convergence rate. A drawback of this approach is the impracticability of assessing the uncertainties.
  The second goal is to assess the predictive uncertainty, which represents the sum of both epistemic and aleatoric uncertainty. In the work of Mullachery et al. (Ref. [16]), the authors take advantage from the so-called BNNs. The model parameters, such as neuron weights, are not represented by single values but by probability distributions. This allows for the quantification of uncertainties, which reflect the inherent limitations in our knowledge of the underlying system. This approach facilitates a more comprehensive understanding of the model predictions and their associated confidence levels.

2.3. Flight Testing

To validate our simulation model, flight tests were successfully performed. Skiron-X was equipped with several sensors, including accelerometers and strain gauges to characterize the structural response of the eVTOL. Maneuvers in both HC and AP modes were conducted trying to cover the whole flight envelope. In this work, the flight test data is used to assess the qualitative response of the FSM.

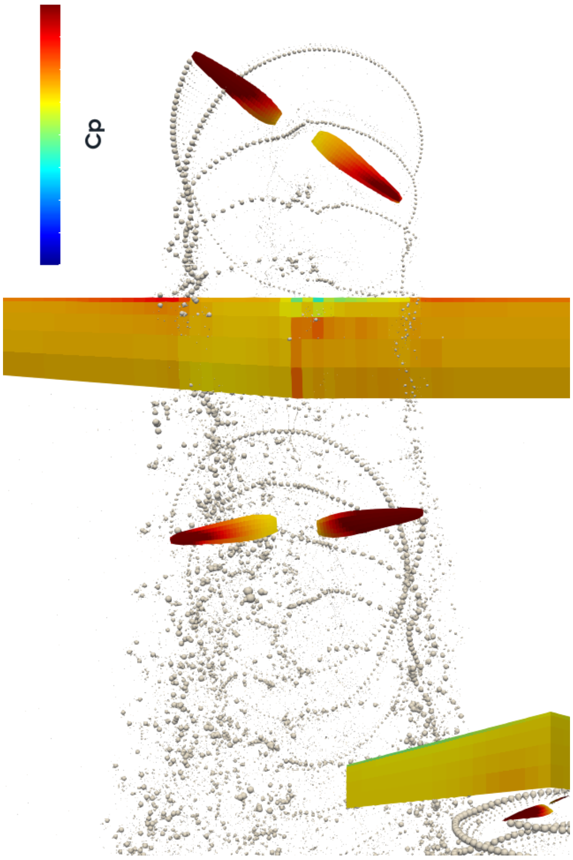

Figure 3: DUST simulation of Skiron-X.

2.4. Uncertainty quantification

One of the most important aspects of this research is the trustworthiness of our DT prediction. A way to interpret it is related to uncertainty quantification (UQ). It is essential to identify regions where predictions could be less reliable due to a scarce amount of data points or high variance. Uncertainties can be divided into two main categories: aleatoric uncertainties and epistemic uncertainties. The former category accounts for the natural variability and randomness of our eVTOL and its environment. Pretending to perfectly know our system would be an unsafe assumption, there are always unknown unknowns that can lead our system to behave unpredictably. Some examples of our eVTOL could be related to manufacturing tolerances or the variability in material properties, such as strength or elasticity. Whereas, concerning the environment, the measurements of pressure and temperature can be not accurate. In this work, this UQ category is not touched, and it could be a possible topic for further investigation.

The second group of UQs are epistemic uncertainties, which are associated with methodological errors. These uncertainties could be reduced by using more complex models that better describe our system or by including more data that characterize particular conditions. From an aerodynamic point of view, they are related to turbulence modelling and flow unsteadiness. To quantify them, GPs and BNNs perfectly fit our needs. As their output consists of a combination of a mean value and its variance, the model predictions' confidence can be assessed easily. Both aleatory and epistemic UQs provide a so-called "confidence interval", which is constructed around a mean prediction and bounded within a certain variance range, usually covering 95% of the possible predictions. Knowing the range size, in which most of the predictions fall, is already a valuable information to make better decisions. The researcher will focus on this aspect to analyze the confidence of the methods and procedures applied and assess if it can be used effectively for other applications, such as certification purposes.

3. ROTORS DATA-DRIVEN MODEL

As explained in the previous section, the ML contribution to our FSM is implemented for the prediction of the rotors' thrusts and moments. The dataset is composed of a large number of LF samples and only a limited number of MF simulation points. A schematic is depicted on Figure 4. The inputs x_{input} are defined by the environmental flight conditions (AOA, angle of sideslip (AOS) and free stream velocity U_∞), and the rotational speed of each propeller N. The AOA varies from -180° to 180°, the AOS from -90° to 90° and U_∞ from 0 m/s to 33 m/s. The rotational speed of the lift and pusher propellers ranges from 0 rpm to 3500 rpm, respectively. On the other hand, the model outputs $\hat{y}_{output}$ are the thrust forces T and propeller torques Q, which are needed for the FSM analysis. The multi-fidelity dataset is created using the LF and MF methods described in Sec. 2.2.1. Subsequently, the data-driven model is trained and validated with the two methods proposed in Sec. 2.2.2.

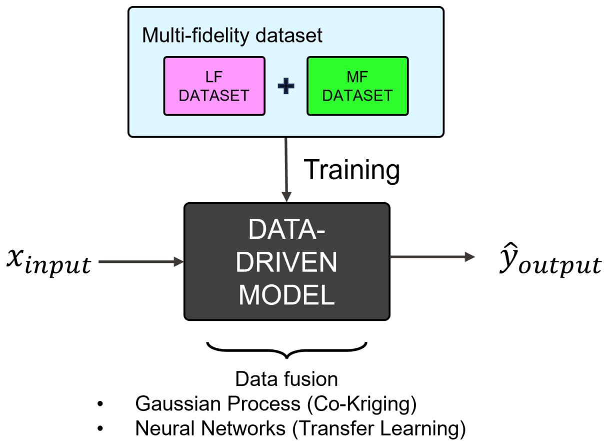

Figure 4: Data-driven diagram representation.

Figure 5 shows the distribution of the dataset in LF (pink) and MF (green). A classical Latin Hypercube Sampling method was used to sample LF points. About 2000 calculation were performed on LF, whereas 60 simulations were run in MF. As it can be noted, the dataset space is mainly divided into two areas, which correspond to the eVTOL AP and HC modes. In the lower fidelity case, the space boundaries were much larger than the real and simulated flight regimes. This would possibly include some non-nominal scenarios such as failures or include the presence of wind gusts.

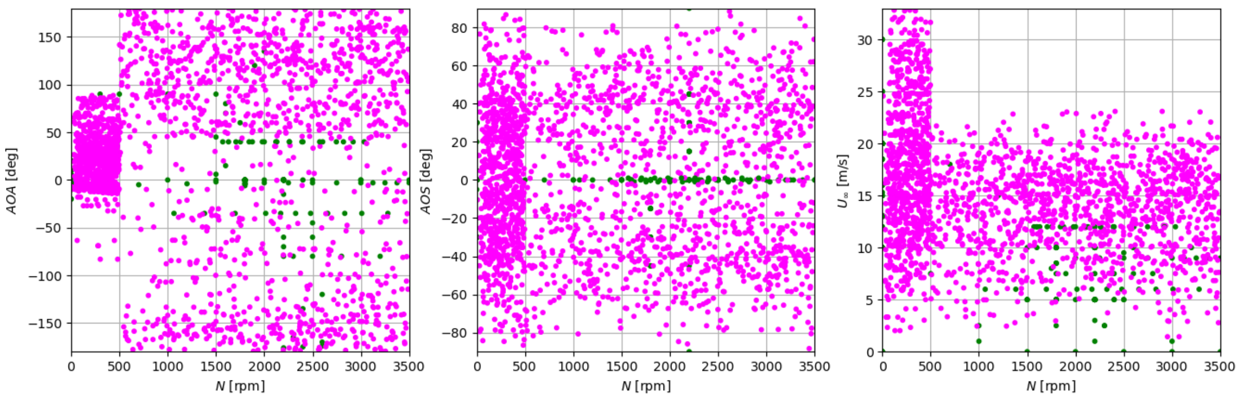

Figure 5: Dataset points distribution of one lift propeller: LF in pink, MF in green.

4. RESULTS AND DISCUSSION

The results are divided into two parts. The first part is about the training and validation of the ML models, while the second illustrates the Flight Mechanics and Aeroelastic modules' results of the complete FSM.

4.1. Data-driven rotor model

Table 1 describes the comparison between the two final ML approaches, the state-of-the-art Co-Kriging and the BNN-TL with as well the two BNN trained with only LF and MF datasets, respectively. It shows the average training time $\bar{t}_{train}$, average prediction time $\bar{t}_{pred}$, percentage average error $\bar{\epsilon}_{tot}$ and percentage average confidence interval $\bar{\sigma}_{tot}$. As expected, the Co-Kriging model is faster for both training and prediction time. However, our BNN-TL model reported a lower error and a better standard deviation, demonstrating the ability to represent the complex system better than the state-of-the-art approach. In addition, a higher confidence interval is an indication of more reliable predictions.

Table 1: Data-driven models comparison.

Model	$\bar{t}_{train}[min]$	$\bar{t}_{pred}[s]$	$\bar{\epsilon}_{tot}[\%]$	$\bar{\sigma}_{tot}[\%]$
BNN-LF	41	0.020	8.5	94.2
BNN-MF	35	0.020	6.4	92.1
BNN-TL	55	0.020	**1.8**	**97.3**
Co-Kriging	**4**	**0.005**	5.9	88.2

In Figure 6, a comparison between multiple BNN models is done. The BNN predictions of the pusher propeller thrust over revolution speed at constant AOA=-5°, AOS=0° and U_∞ are shown. The pink, green and blue curves depict the output of BNN-LF, BNN-MF and BNN-TL models. These models represent respectively the three hyperparameter-optimized models trained on solely LF, MF datasets while BNN-TL uses both LF and MF with TL. In addition, the black stars illustrate the validation points, i.e. some points that are part of the dataset but are not used for the training. From Figure 6 it is also clear that BNN-LF follows an overestimated curve and BNN-MF convergence is poor due to a low number of samples. On the other hand, the BNN-TL gives the best overall reliable thrust prediction, having the smallest standard deviation band and being closer to the validation points. This demonstrates that the data fusion method based on TL is more reliable and accurate compared to the use of models trained on single fidelity datasets separately. For this reason, the BNN-TL rotors model was chosen to be integrated into the FSM.

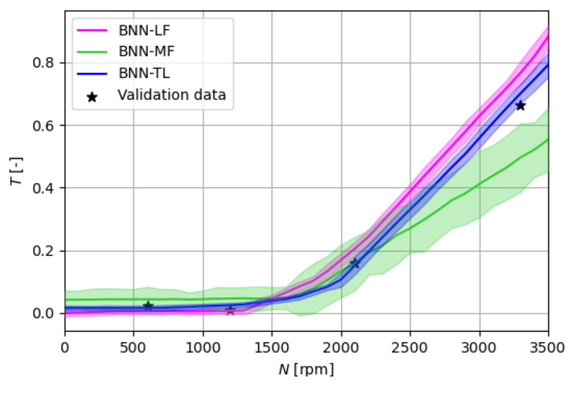

Figure 6: Comparison between different ML methods: BNN-LF (pink), BNN-MF (green) and BNN-TL (blue). Thrust T is normalized with the maximum propeller force.

4.2. Flight Simulation Model analysis

The following section is about the results obtained from the FSM with and without the integration of the BNN-TL model, here indicated as FSM-LF and FSM-BNN-TL. In addition a comparison with flight test data is also available.

4.2.1. Flight Mechanics Module

Trim conditions

Figure 7 shows the pusher propeller rpm N, elevator deflection δ_{DE} and wing root bending moment M_B in various trim conditions. The values were obtained from flight test data, as well as from the FSM, both with and without integration of the BNN-TL module for propeller thrust described in section 3. Flight test data points were averaged during four different flight conditions: straight and level flight (orange), and leveled coordinated turns with a varying radius of 95 m (blue), 150 m (green) and 330 m (red). It can be seen that both the trim elevator deflection as well as the wing root bending moment with and without BNN-TL module are very similar at all airspeeds and trim conditions. This can be explained by the fact that the BNN-TL module only affects the propeller thrust and torque, and not the remaining aerodynamics or the structural model. In fact, a known deficit of the LF aerodynamic model was the underestimation of the vehicle's parasitic drag. This causes an underestimation in both the required thrust and rpm to trim the FSM. Neither the LF aerodynamics, thrust or structural models were tuned to fit the flight test data, which explains the corresponding biases in the trim results. No flight test data was used in the training of the BNN-TL module either. Nevertheless, the results show that both model predict plausible trim conditions.

Dynamic flight

This section presents a comparison of the FSM with the initial LF rotors model (FSM-LF) and with the integrated BNN-TL rotors model (FSM-BNN-TL). The goal is to assess the advantages earned from the ML contribution, expected to be more visible during the transition phase. The authors are aware that the FCS plays a significant role in the eVTOL behaviour. For the sake of simplicity, exactly the same logic was employed in both models.

Figure 8 shows three graphs of a typical transition from HC to AP mode over simulation time. The first chart represents the eVTOL true airspeed (TAS). It increases from 0 m/s in HC mode, i.e. eVTOL in hovering, to a typical cruise speed in AP mode. The results from the FSM-LF and FSM-BNN-TL are displayed in dashed and solid lines, respectively. This figure can be used to identify the eVTOL state during the transition phase.

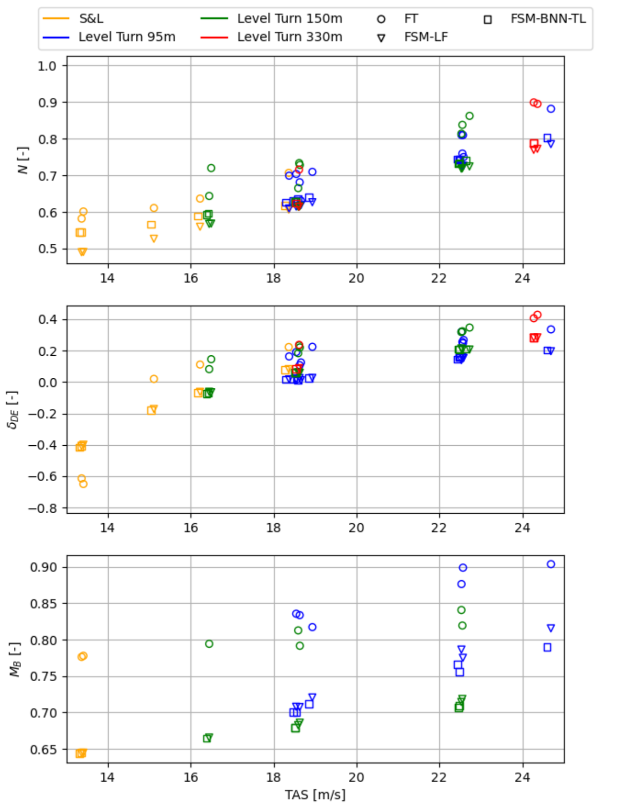

Figure 7: FSM trim points comparison: pusher propeller rpm N_{pp} (top), elevator deflection δ_{DE} (mid) and wing root bending moment M_B (bottom) over TAS. Results are normalized with respect to their operational ranges.

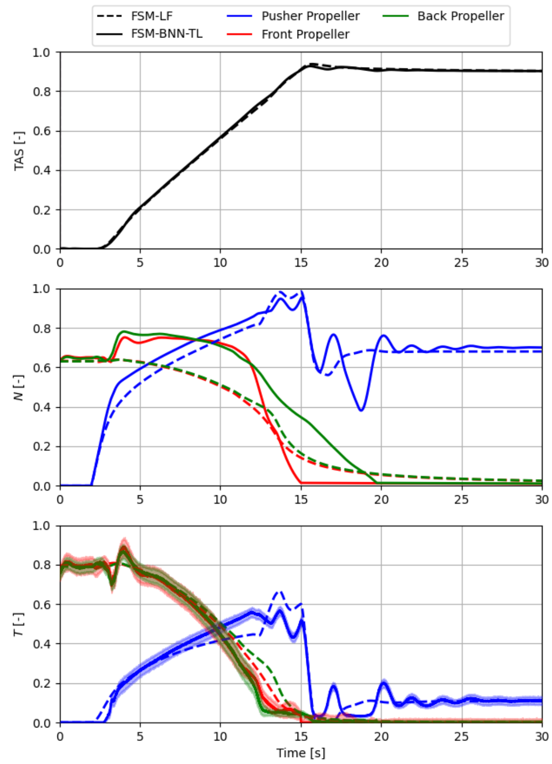

Figure 8: FSM dynamic simulation of a transition between HC and AP mode: TAS, rotational speed N and propeller thrust T are depicted. Results are normalized with respect to their operational ranges.

The second graph shows the rotational speed of the pusher propeller (blue) and the left front (red) and back (green) propellers. During this maneuver, the pusher propeller difference between LF and BNN-TL is minimal. Only a discrepancy is noted right after the eVTOL reaches the cruise speed, where the FCS of the FSM-BNN-TL correct the pusher propeller N_{PP} and brings it to a stable condition.

On the other hand, a much more interesting comparison is found between the front and back propeller behavior. In the LF case (dashed red and green lines), the rotational speed difference is minimal. However, when the simulation is performed with the BNN-TL (solid red and green lines), the difference between the two propeller is evident and it seems to increase with increase in airspeed. The BNN-TL rotors model is taking into account the detrimental effects caused by the wake shedding. In fact, the back propeller N_{BP} is greater than the front propeller N_{FP} to compensate the thrust drop caused by the front rotor and wing wakes. This is confirmed by the third figure, which depicts the rotors thrust with the confidence interval. Between 12 and 20 seconds the rpm difference between N_{BP} and N_{FP} starts to be important, while the thrust predicted is similar. The back propeller thrust reduction derives from the MF simulations which model and capture the wake effects.

The third figure gives another interesting finding attributed to the standard deviation. In general, it is reported to be larger during the transition itself, i.e. between 3 and 20 seconds. In that region, the BNN-TL model seems to be less confident and the FSM user should pay more attention on the result evaluation.

4.2.2. Aeroelastic Module

The Aeroelastic module includes the elastic and rigid degrees of freedom of a FEM of the aircraft. The FEM is built with beam elements and tuned to match the modes and natural frequencies obtained from a ground vibration test. The aerodynamic forces are modelled using a state-space approach inspired to Leishman [17], whereas the steady values of the rotor thrust is obtained from the Flight Mechanics module. As such, the model can be used in time domain to calculate the nonlinear dynamic response and linearized and used to assess linear stability and dynamic response in the frequency domain.

Figures 9 and 10 display a radar plot comparing the Root Mean Square (RMS) values of the wing bending moments and CG accelerations, respectively, derived from the reduced-order model predictions and experimental data across different flight points. The perturbations are composed of discrete gusts, the magnitude of which has been broadly tuned to match both bending moments and accelerations.

The blue line represents the model predictions, while the black line with star markers denotes the experimental results. The shaded area within the radar plot emphasizes regions of higher RMS bending moments, identifying critical points for structural integrity assessment under turbulent and gusty conditions. This plot provides a clear visual representation of the model accuracy in replicating real-world scenarios, demonstrating its validity and reliability.

Figure 11 offers a comprehensive view of the system aeroelastic stability and frequency response through V-g plots in HC and AP mode, respectively. The top subplot illustrates the damping (ξ/ω_{ref}) variation with respect to the normalized velocity (U/U_{ref}). This subplot is crucial for identifying the critical speeds where the system damping approaches zero, indicating the onset of flutter or other instabilities. The bottom subplot shows the frequency (f/f_{ref}) versus normalized velocity (U/U_{ref}). This plot highlights the variation of the model frequencies, a phenomenon where different modal frequencies may potentially coalesce as the velocity increases, further indicating potential instability regions.

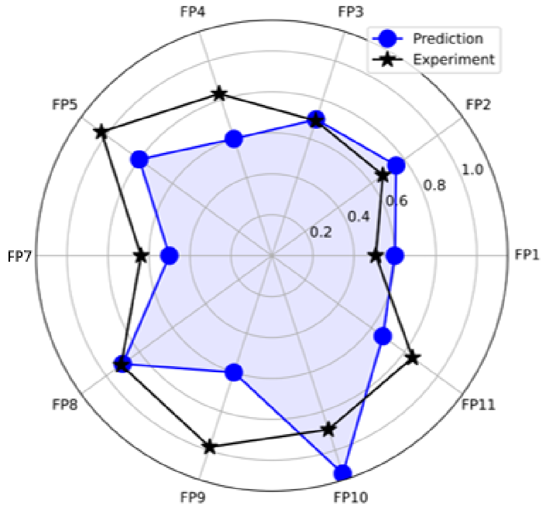

Figure 9: Wing Bending Moment RMS.

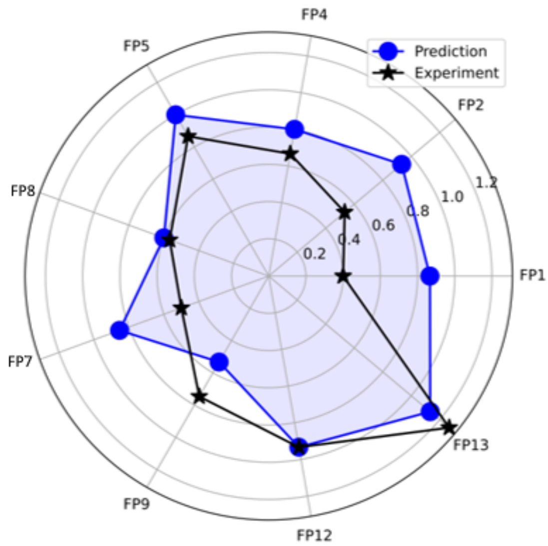

Figure 10: CG acceleration RMS.

Figure 12 present root locus plots in HC and AP mode, respectively, which provides the same information as the previous image but in a format (imaginary part versus the real part of the eigenvalues) which can more readily highlight the mechanisms at the origin of the unstable modes (refer to [18] and to [19] for a more comprehensive presentation of the topic). All in all, the aeroelastic analysis does not identify any instability nor does it highlight any unexpected behavior.

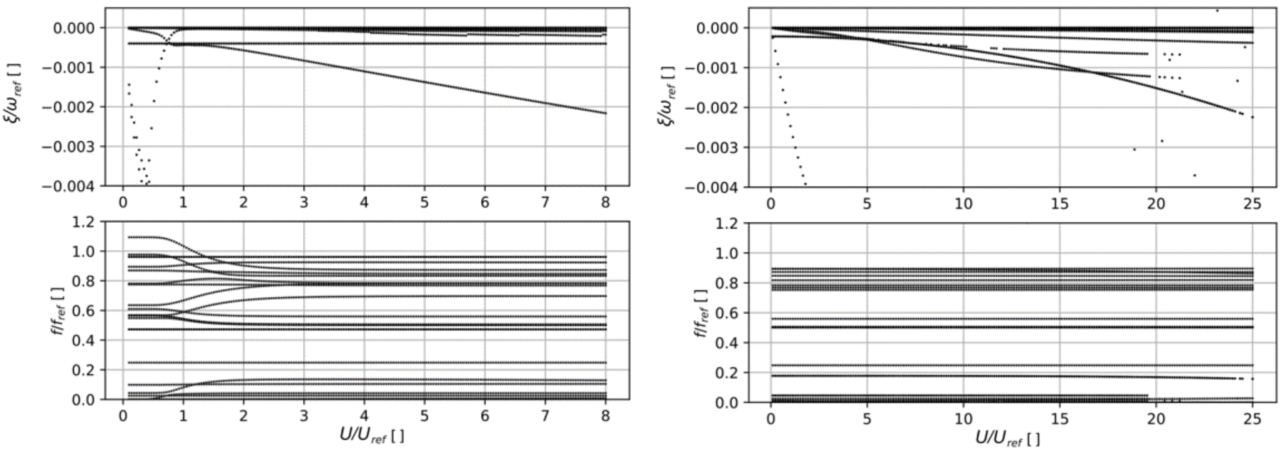

Figure 11: V-g plots in HC (left) and AP mode (right).

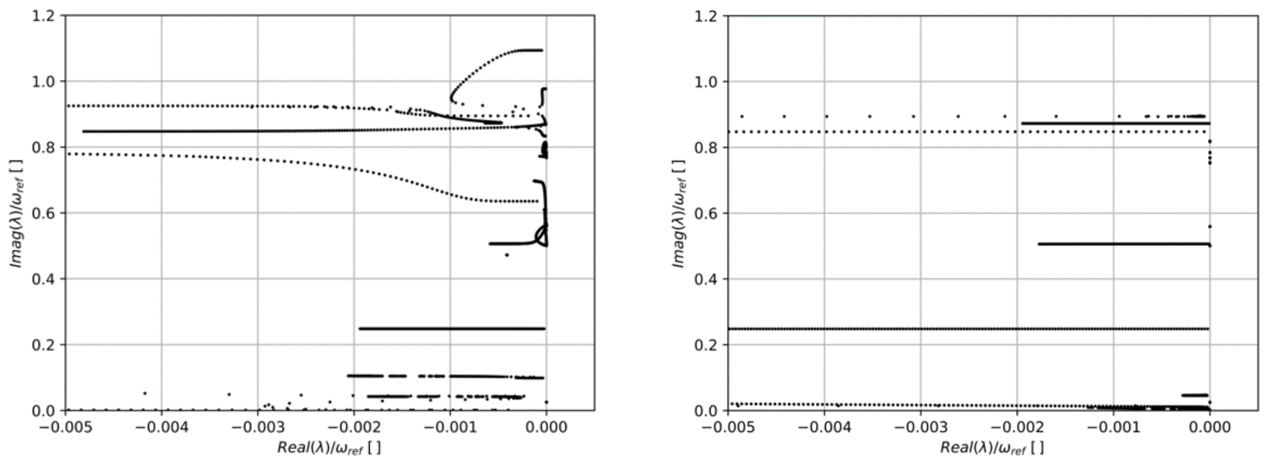

Figure 12: Root locus in HC (left) and AP mode (right).

5. CONCLUSIONS

In the framework of the Horizon Europe project MODEL-SI, the authors focused on developing a DT of an eVTOL machine as a case study to assess the suitability for certification purposes. The final model is a FSM of the drone Skiron-X of Aurora Flight Sciences. The model is able to perform a wide range of static and dynamic analyses. These include calculating aircraft trim for steady flight conditions, simulating the critical transition phase between HC and AP modes, and conducting aeroelastic analyses to assess how the eVTOL structure responds to aerodynamic loads. This can include studying how the structure bends and twists under different flight conditions.

The model addresses the complexity of rotor and wing aerodynamics by adopting data-driven multi-fidelity techniques. The accuracy and robustness of this approach are enhanced by the use of ML methods, which also provide an indication of the model's uncertainties. A data-driven model for all rotors is implemented and was tested with both Co-Kriging and BNN-TL techniques. The former provide a simpler and faster implementation, in fact, an average training time of one order of magnitude less than the BNN approach is reported. However, the latter showed better prediction capabilities with an average error $\bar{\epsilon}_{tot}$=1.8%.

While ML is not strictly necessary for this approach, it significantly improves the system's ability to handle realistic scenarios. This is confirmed from our results of Sec. 4. Firstly, the FSM is compared to FT data collected with Skiron-X. Both FSM with and without integration of the propellers BNN-TL model outputs were analyzed. In general, both models show a similar trend to FT data. Finally, the improvement of the FSM using the ML component was shown in Sec. 4.2.1, where a transition from HC to AP mode is analyzed. Here the FSM with integrated BNN-TL model for propeller thrust showed a more realistic behavior. During the transition, the back propeller thrust reduces with respect to the airspeed due to the front propeller and wing wakes which create a non-ideal perturbed inflow condition.

Even though our model pertains to a 22 kg drone, the complexity of the physics involved is comparable to that of larger eVTOL aircraft. We find our results encouraging and believe that the proposed approach has significant potential.

Author contacts:

Andrea Pedrioli, andrea.pedrioli@zhaw.ch
Andrea Vaiuso, andrea.vaiuso@zhaw.ch
Noé Pedrazzini, noe.pedrazzini@zhaw.ch
Oier Coretti, oier.coretti@zhaw.ch
Elena Garcia Sanchez, elena-beatriz.garcia-sanchez@easa.europa.eu
Laurent Pinsard, laurent.pinsard@easa.europa.eu
Joana Vieira Gomes, joana.gomes@easa.europa.eu
Pierluigi Capone, pierluigi.capone@zhaw.ch
Marcello Righi, marcello.righi@zhaw.ch

6. ACKNOWLEDGMENTS

The MODEL-SI project received funding from the European Union's Horizon Europe research and innovation programme. The authors wish to acknowledge the support of MODEL-SI project team and in particular to Moreno Apicella, Gabriele Immordino, Dr. Xinying Liu and David Anderegg. A special thanks to the Aurora Flight Sciences team that contributed to the flight testing activities: Angelo Esposito, Andrew Heafitz, Roger Titshall.

7. REFERENCES

[1] A. Pedrioli, P. Capone, M. Righi, E. Garcia-Sanchez, L. Pinsard, and J. V. Gomes, "MODEL-SI: Modeling and Simulation - Multi-fidelity surrogate model of an eVTOL for certification," in *AIAA SCITECH 2024 Forum*, Orlando (FL): American Institute of Aeronautics and Astronautics, Jan. 2024. DOI: https://doi.org/10.2514/6.2024-1624.

[2] A. Cocco and A. Savino, "Tiltrotor Whirl-Flutter Assessment by Multifidelity Aerodynamic Models," en, in *AIAA SCITECH 2024 Forum*, Orlando, FL: American Institute of Aeronautics and Astronautics, Jan. 2024, ISBN: 978-1-62410-711-5. DOI: 10.2514/6.2024-1850.

[3] A. Vaiuso, G. Immordino, M. Righi, and A. D. Ronch, *Multi-fidelity bayesian neural network for uncertainty quantification in transonic aerodynamic loads*, 2024. arXiv: 2407.05684 [cs.CE]. [Online]. Available: https://arxiv.org/abs/2407.05684.

[4] USDOD, "Flying qualities of piloted aircraft. mil. stand. mil-std-1797a (notice 3)," 2004.

[5] M. Drela, *Flight vehicle aerodynamics*, en. Cambridge (Mass.): MIT press, 2014, ISBN: 978-0-262-52644-9.

[6] H. Glauert, *The Elements of Aerofoil and Airscrew Theory* (Cambridge Science Classics), Second. Cambridge: Cambridge University Press, 1947, ISBN: 978-0-521-27494-4. DOI: 10.1017/CBO9780511574481. (visited on 06/09/2023).

[7] D. Peters and N. Haquang, "Dynamic inflow for practical applications," *Journal of the American Helicopter Society*, vol. 33, no. 4, pp. 64–68, Oct. 1988. (visited on 06/01/2023).

[8] E. Oñate, *Structural Analysis with the Finite Element Method Linear Statics* (Lecture Notes on Numerical Methods in Engineering and Sciences), en, E. Oñate, Ed. Dordrecht: Springer Netherlands, 2013, ISBN: 978-1-4020-8742-4 978-1-4020-8743-1. DOI: 10.1007/978-1-4020-8743-1. [Online]. Available: http://link.springer.com/10.1007/978-1-4020-8743-1 (visited on 06/05/2023).

[9] T. Theodorsen and I. E. Garrick, "Nonstationary flow about a wing-aileron-tab combination including aerodynamic balance," National Advisory Committee for Aeronautics, REPORT No.736, 1942.

[10] T. Theodorsen, "General Theory of Aerodynamic Instability and the Mechanism of Flutter," National Advisory Committee for Aeronautics, Tech. Rep. REPORT No.496, 1949.

[11] M. Karpel, "Size-Reduction Techniques for the Determination of Efficient Aeroservoelastic Models," en, in *Control and Dynamic Systems*, vol. 54, Elsevier, 1992, pp. 263–295, ISBN: 978-0-12-012754-2. DOI: 10.1016/B978-0-12-012754-2.50011-X. [Online]. Available: https://linkinghub.elsevier.com/retrieve/pii/B978012012754250011X (visited on 07/17/2024).

[12] B. Davoudi and K. Duraisamy, "A Hybrid Blade Element Momentum Model for Flight Simulation of Rotary Wing Unmanned Aerial Vehicles," in *AIAA Aviation 2019 Forum*, Dallas, Texas: American Institute of Aeronautics and Astronautics, Jun. 2019, ISBN: 978-1-62410-589-0. DOI: 10.2514/6.2019-2823. (visited on 01/19/2024).

[13] *Dust gitlab page*, https://public.gitlab.polimi.it/DAER/dust, Accessed: 2024-07-10, 2024.

[14] C. E. Rasmussen, C. K. Williams, *et al.*, *Gaussian processes for machine learning*. Springer, 2006, vol. 1.

[15] K. Kontolati, P. Tsilifis, S. Ghosh, V. Andreoli, M. Shields, and L. Wang, "Multi-fidelity metamodeling in turbine blade airfoils via transfer learning on manifolds," in *AIAA SCITECH 2023 Forum*, 2023, p. 0918.

[16] V. Mullachery, A. Khera, and A. Husain, *Bayesian neural networks*, 2018. arXiv: 1801.07710 [cs.LG]. [Online]. Available: https://arxiv.org/abs/1801.07710.
[17] J. Leishman and K. Nguyen, "State-space representation of unsteady airfoil behavior," *AIAA journal*, vol. 28, no. 5, pp. 836–844, 1990.
[18] R. L. Bisplinghoff, H. Ashley, and R. L. Halfman, *Aeroelasticity*. Courier Corporation, 2013.
[19] E. H. Dowell, *A modern course in aeroelasticity*. Springer, 2014, vol. 217.